

DFTT 47/97
 PSI-PR-97-18
 October 1997
 hep-ph/9710375

QCD corrections to $e^+e^- \rightarrow u \bar{d} s \bar{c}$ at Lep 2 and the Next Linear Collider: CC11 at $\mathcal{O}(\alpha_s)$.¹

Ezio Maina^a, Roberto Pittau^b and Marco Pizzio^a

^a*Dip. di Fisica Teorica, Università di Torino and INFN, Sezione di Torino,
 v. Giuria 1, 10125 Torino, Italy.*

^b*Paul Scherrer Institute
 CH-5232 Villigen-PSI, Switzerland*

Abstract

QCD one-loop corrections to the full gauge invariant set of electroweak diagrams describing the hadronic process $e^+e^- \rightarrow u \bar{d} s \bar{c}$ are computed. Four-jet shape variables for WW events are studied at next-to-leading order and the effects of QCD corrections on the determination of the W -mass in the hadronic channel at Lep 2 and NLC is discussed. We compare the exact calculation with a “naive” approach to strong radiative corrections which has been widely used in the literature.

¹ Work supported in part by Ministero dell' Università e della Ricerca Scientifica.

Introduction

The measurement of W -mass to high precision is one of the main goals of Lep 2 and will provide a stringent test of the Standard Model (SM) [1, 2]. In fact, the mass of the W boson in the SM is tightly constrained and an indirect determination of M_W can be obtained from a global fit of all electroweak data. The fit gives [3] $M_W = 80.338 \pm 0.040_{-0.018}^{+0.009}$ GeV where the central value corresponds to $M_H = 300$ GeV and the second error reflects the change of M_W when the Higgs mass is varied between 60 and 1000 GeV. A disagreement between the value of M_W derived from the global fit and the value extracted from direct measurement would represent a major failure of the SM. Alternatively, an improvement in the value of the W -mass can significantly tighten present bounds on the Higgs mass. These studies will be continued and improved at the Next Linear Collider (NLC) which is expected to reduce the error on the measurement of W -mass down to about 15 MeV [4].

In order to extract the desired information from WW production data, theoretical predictions with uncertainties smaller than those which are foreseen in the experiments are necessary. This requires a careful study of all radiative corrections which have to be brought under control. In this paper we will be concerned with QCD corrections which are known [5, 6] to modify the shape of the W -mass peak and the distributions of others kinematical variables. Since event shape variables are often used to extract WW production from the background it is highly desirable to have a complete next-to-leading order (NLO) study of these distributions for WW events. Furthermore, calculations of QCD corrections to $\mathcal{O}(\alpha^2\alpha_s^2)$ four-jet production have recently appeared [7]. Combining these results with a complete calculation of QCD corrections to all $\mathcal{O}(\alpha^4)$ four-fermion processes it would be possible to obtain NLO predictions for any four-jet shape variable at Lep 2 and NLC providing new means of testing perturbative QCD.

W -pair production can result in a variety of four-fermion hadronic final states. The simplest one is $u \bar{d} s \bar{c}$. A gauge invariant description of $e^+e^- \rightarrow u \bar{d} s \bar{c}$ requires in the unitary gauge the eleven diagrams shown in fig. 1. This amplitude is known as CC11 in the literature. The subset of three diagrams labeled (e) and (f) in fig. 1, in which both intermediate W 's can go on mass-shell, is known as CC03 and is often used for quick estimates of WW production. Numerically the total cross sections obtained from CC03 and those obtained from CC11 at Lep 2 and NLC energies differ by a few per mil [8]. Other final states to which W -pairs can decay are $u \bar{u} d \bar{d}$ ($c \bar{c} s \bar{s}$) and, through CKM mixing, $u \bar{u} s \bar{s}$ ($u \bar{u} b \bar{b}$, $c \bar{c} d \bar{d}$, $c \bar{c} b \bar{b}$). The additional diagrams which appear in these latter sets contribute at most at the per-mil level to the total cross section and tend to produce events which resemble very little WW or even single- W events since only electroweak neutral virtual vector bosons appear in them. There are also four-quark final states where only neutral intermediate vector boson, including gluons, play a role like $u \bar{u} c \bar{c}$, $d \bar{d} s \bar{s}$ ($d \bar{d} b \bar{b}$, $s \bar{s} b \bar{b}$), $u \bar{u} u \bar{u}$ ($c \bar{c} c \bar{c}$) and $d \bar{d} d \bar{d}$ ($s \bar{s} s \bar{s}$, $b \bar{b} b \bar{b}$). An additional important contribution to four-jet production, indistinguishable from four-quark events, originates from $e^+e^- \rightarrow q \bar{q} g g$.

In this letter we present the complete calculation of QCD corrections to CC11. While this is only a first step in the calculation of all $\mathcal{O}(\alpha^4)$ four-fermion processes at

NLO, this reaction includes the most important source of background, namely single W production, providing a natural setting for a first study of the role of QCD corrections to gauge invariant sets of four-quark production diagrams.

In most instances QCD corrections have been included “naively” with the substitution $\Gamma_W \rightarrow \Gamma_W(1 + 2/3 \alpha_s/\pi)$ and multiplying the hadronic branching ratio by $(1 + \alpha_s/\pi)$. This prescription is exact for CC03 when fully inclusive quantities are computed. However, it can only be taken as an order of magnitude estimate even for CC03 in the presence of cuts on the jet directions and properties, as discussed in [5]. It is well known that differential distributions can be more sensitive to higher order corrections than total cross-sections in which virtual and real contributions tend to cancel to a large degree. It is therefore necessary to include higher order QCD effects into the predictions for WW production and decay in a way which allows to impose realistic cuts on the structure of the observed events. The impact of QCD corrections on the angular distribution of the decay products of a W and their application to on-shell W -pair production is discussed in ref. [9].

Calculation

One-loop virtual QCD corrections to $e^+e^- \rightarrow u \bar{d} s \bar{c}$ are obtained by dressing all diagrams in fig. 1 with gluon loops. Defining suitable combinations of diagrams one can organize all contributions in a very modular way [6]. All QCD virtual corrections to $\mathcal{O}(\alpha^4)$ four-fermion processes can be computed using the resulting set of loop diagrams.

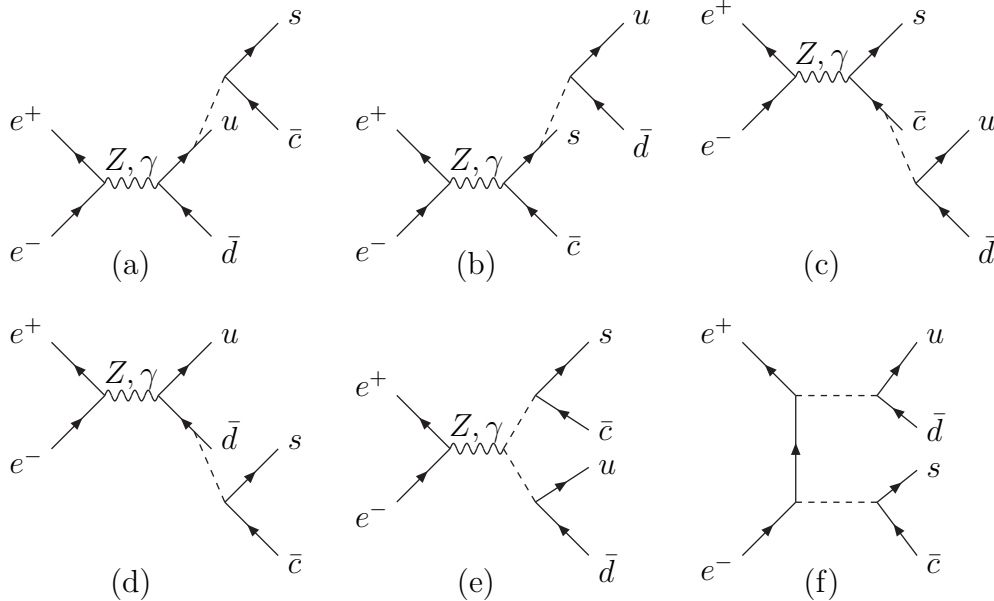


Figure 1: Tree level diagrams for $e^+e^- \rightarrow u \bar{d} s \bar{c}$. The dashed lines are W 's.

The real emission contribution for $e^+e^- \rightarrow u \bar{d} s \bar{c}$ can be obtained attaching a gluon to the quark lines of the diagrams shown in fig. 1 in all possible positions. This

results in fifty-two diagrams. The required matrix element has been computed using the formalism presented in ref. [10] with the help of a set of routines (PHACT) [11] which generate the building blocks of the helicity amplitudes semi-automatically.

The calculation of the virtual corrections has been performed in two different ways, with identical results. In the first case we have used the standard Passarino–Veltman [12] reduction procedure, while in the second we have used the new techniques presented in [13]. The matching between real and virtual corrections has been implemented as in [6], using the dipole formulæ of ref. [14]. All integrations have been carried out using the Monte Carlo routine VEGAS [15].

An important ingredient for accurate predictions of W -pair production is the effect of initial state radiation (ISR). In the absence of a calculation of all $\mathcal{O}(\alpha)$ corrections to four-fermion processes, these effects can only be included partially. In contrast with Lep 1 physics a gauge invariant separation of initial and final state radiation is not possible. Only the leading logarithmic part of ISR is gauge invariant and universal. These contributions can be included using structure functions. Part of the non-logarithmic terms have been computed for CC03 and some other final states in [16] using the *current splitting technique* [17]. This corresponds to splitting the electrically neutral t -channel neutrino flow into two oppositely flowing charges, assigning the -1 charge to the initial state and the $+1$ charge to the final state. In this way a gauge-invariant definition of ISR can be given. However, there are clearly cancellations between initial and final state radiation whose relevance is difficult to estimate in the absence of a complete calculation. Quite recently the full calculation of all $\mathcal{O}(\alpha)$ corrections to $e^+e^- \rightarrow W^+\mu\bar{\nu}_\mu$ has been published [19]. Non factorizable QED corrections to CC03 have been studied in [20]. We have only included the leading logarithmic part of ISR using the β prescription in the structure functions, where $\beta = \ln(s/m^2) - 1$. Beamstrahlung effects have been ignored. We have not included Coulomb corrections to CC03, which are known to have a sizable effect, particularly at threshold. They could however be introduced with minimal effort.

Results

In this section we present a number of cross sections and distributions for $e^+e^- \rightarrow u\bar{d}s\bar{c}$. We have used $\alpha_s = .123$ at all energies. ISR is included in all results. The width of the W -boson is kept fixed and includes $\mathcal{O}(\alpha_s)$ corrections.

For the Lep 2 workshop [1] the so called ADLO/TH set of cuts have been agreed on:

- the energy of a jet must be greater than 3 GeV;
- two jets are resolved if their invariant mass is larger than 5 GeV;
- jets can be detected in the whole solid angle.

For the NLC a slightly different set called NLC/TH has been chosen. The NLC/TH set of cuts differs from the ADLO/TH set in that a minimum angle of 5° is required

	$E_j > 3 \text{ GeV}, y_D = 0.01$	$E_j > 3 \text{ GeV}, y_D = 0.01,$ $ M_{Ri} - M_W < 10 \text{ GeV}$	$E_j > 3 \text{ GeV}, y_D = 0.01,$ $ M_{Ri} - M_W < 10 \text{ GeV},$ smeared
NLO	1.1493(4)	0.7895(5)	0.7758(9)
nQCD	1.1069(3)	1.0545(3)	1.0479(3)

Table I: Cross sections in pb at $\sqrt{s} = 175 \text{ GeV}$.

between a jet and either beam (as appropriate for the larger bunch size at the NLC and the corresponding larger bunch disruption at crossing) and that two jets are resolved if their invariant mass is larger than 10 GeV. Both set of cuts will also be referred to as “canonical” in the following. We have preferred a different criterion for defining jets which is closer to the actual practice of the experimental collaborations. For mass reconstruction studies we have used the Durham scheme [18], with $y_D = 1. \times 10^{-2}$ at Lep 2 energies. At the NLC we have adopted a smaller cut $y_D = 1. \times 10^{-3}$ in order to have an adequate fraction of events with at least four jets. The four-momenta of the particles which have to be recombined have been simply summed. If any surviving jet had an energy smaller than 3 GeV it was merged with the jet closest in the Durham metric.

Previous studies [8] have shown that the differences between the total cross sections obtained from CC11 and those obtained with CC03 are at the per mil level. Much larger effects have been found in observables like the average shift of the mass reconstructed from the decay products from the true W -mass.

In fig. 2 we compare the NLO spectrum of the average reconstructed W -mass with the naive-QCD (nQCD) result at Lep 2 energies. All events with at least four observed jets have been retained in fig. 2. The two candidate masses are obtained forcing first all remaining five-jet events to four jets, merging the two partons which are closest in the Durham scheme, and then selecting the two pairs which minimize

$$\Delta'_M = (M_{R1} - M_W)^2 + (M_{R2} - M_W)^2. \quad (1)$$

where M_{R1} and M_{R2} are the two candidate reconstructed masses and M_W is the input W -mass.

In fig. 2 the dashed line refers to the nQCD results while those of the full NLO calculation are given by the continuous line. The corresponding cross section are given in table I. Fig. 2a is obtained using only the basic set of cuts described above. Since all experiments restrict their analysis to a region around the expected W -mass, we have studied the effect of requiring that both reconstructed masses lie within 10 GeV of the input mass. The result is shown in fig. 2b. Finally we have tried to take into account some form of experimental smearing, in order to determine whether the distortion of the mass distribution we observe does survive in a more realistic setting. To this aim we have smeared the reconstructed masses entering eq. (1), using a gaussian distribu-

tion with a 2 GeV width. This procedure gives fig. 2c. It is worth mentioning that simulating experimental smearing at NLO is far more complicated than at tree level. In order to preserve the delicate cancellations between the real emission cross section and the subtraction terms, both contributions to four-jet quantities must be smeared, event by event, by the same amount. Fig. 2 shows that at NLO the mass distribution is shifted towards lower masses and a long tail for rather small average masses is generated, with a corresponding reduction of the high-mass part of the histogram. This tail is eliminated when only reconstructed masses in the vicinity of the expected W -mass are retained. Even with this additional cut, however, the NLO distribution is clearly different from the nQCD one. The reduction in cross section (see Table I) shows that a large number of soft gluons is exchanged, at the perturbative level, between decay products of different W 's. In our simplified treatment of experimental uncertainties these differences are still visible though somewhat reduced. If we try to quantify the mass shift using the standard quantity:

$$\langle \Delta M \rangle = \frac{1}{\sigma} \int \left(\frac{M_{R1} + M_{R2} - 2M_W}{2} \right) d\sigma. \quad (2)$$

we obtain $\langle \Delta M \rangle_{NLO} = -0.229(1)$ GeV and $\langle \Delta M \rangle_{nQCD} = -0.0635(4)$ GeV when both reconstructed masses are required to lie within 10 GeV of the input mass $M_W = 80.23$ GeV and no smearing is applied.

In fig. 3 we compare the NLO spectrum of the average reconstructed W -mass with the naive-QCD (nQCD) result at the NLC, using the procedure already described for the Lep 2 case but for a smaller minimum Durham cut $y_D = 1. \times 10^{-3}$. Because of the larger relative momentum of the two W 's it is less likely that partons from the decay of one W end up close to the decay products of the other W -boson, therefore the difference between the two distributions is smaller than at Lep 2 energies.

In fig. 4 we present the distributions at $\sqrt{s} = 175$ GeV of the following four-jet shape variables [21]:

- the Bengtsson-Zerwas angle: $\chi_{BZ} = \angle[(\mathbf{p}_1 \times \mathbf{p}_2), (\mathbf{p}_3 \times \mathbf{p}_4)]$ (fig. 4a);
- the Körner-Schierholz-Willrodt angle :
 $\Phi_{KSW} = 1/2\{\angle[(\mathbf{p}_1 \times \mathbf{p}_4), (\mathbf{p}_2 \times \mathbf{p}_3)] + \angle[(\mathbf{p}_1 \times \mathbf{p}_3), (\mathbf{p}_2 \times \mathbf{p}_4)]\}$ (fig. 4b);
- the angle between the two least energetic jets; $\alpha_{34} = \angle[\mathbf{p}_3, \mathbf{p}_4]$ (fig. 4c);
- the (modified) Nachtmann-Reiter angle: $\theta_{NR}^* = \angle[(\mathbf{p}_1 - \mathbf{p}_2), (\mathbf{p}_3 - \mathbf{p}_4)]$ (fig. 4d).

The numbering $i = 1 \dots, 4$ of the jet momenta \mathbf{p}_i corresponds to energy-ordered four-jet configurations ($E_1 > E_2 > E_3 > E_4$). We compare the exact NLO results with the distributions obtained in nQCD and with the results obtained at tree level from the standard background reactions $e^+e^- \rightarrow q \bar{q} g g$, which is the dominant contribution, and $e^+e^- \rightarrow q_1 \bar{q}_1 q_2 \bar{q}_2$.

In all subplots of fig. 4 the full NLO results are given by the continuous line and the nQCD prediction is given by the dashed line. The $q \bar{q} g g$ and $q_1 \bar{q}_1 q_2 \bar{q}_2$ tree level background distributions are given by the chain-dotted and the dotted line respectively.

The shape variables are computed following the procedure outlined in ref. [22] where the Durham cluster algorithm is complemented by the E0 recombination scheme, namely if the two particles i and j are merged the pseudo-particle which takes their place remains massless, with four-momentum:

$$E_{new} = E_i + E_j, \quad \mathbf{p}_{new} = \frac{E_i + E_j}{|\mathbf{p}_i + \mathbf{p}_j|}(\mathbf{p}_i + \mathbf{p}_j). \quad (3)$$

Using this clustering procedure all five-jet events are converted into four-jet events, then each event is used in the analysis if $\min_{i,j=1,4} y_{ij} > y_{cut}$ with $y_{cut} = 0.008$.

In [22] it has been shown that standard parton shower Monte Carlo programs like JETSET do not reproduce well the observed distribution of four-jet shape variables at Lep, which are instead well described by HERWIG 5.9A which includes four parton matrix elements. The discrepancy can be partially explained by the different distributions for the $q \bar{q} g g$ and the $q_1 \bar{q}_1 q_2 \bar{q}_2$ final states, which can be clearly seen in fig. 4, since the four quark final state is included in the parton shower programs only partially. It is precisely in correspondence with the peaks of the $q_1 \bar{q}_1 q_2 \bar{q}_2$ distributions that the discrepancy between data and simulations is larger.

From fig. 4 it is apparent that at NLO four-jet shape variables distributions are significantly modified with respect to leading order results, which are indistinguishable from the nQCD distributions. It is also evident that four-jet distributions in WW events are markedly different from the background distributions and can be useful in separating the two samples. At Lep 2 energies the Körner-Schierholz-Willrodt angle Φ_{KSW} seems to be the most effective variable for this purpose, while the angle between the two least energetic jets α_{34} is of little use, being almost flat over the whole range for all samples. From our results, namely if we assume that the tree level background distributions closely resemble the actual behaviour of the background², it appears that the differences between CC11 distributions and the dominant $q \bar{q} g g$ background decrease when NLO corrections to CC11 are included.

It should be stressed that four-jet shape variables in WW events measure the correlations between the hadronic decays of the two W 's and therefore it should be explicitly checked whether existing codes, NLO calculations or parton shower Monte Carlo programs, successfully reproduce the experimental curves.

The shape-variable distributions at $\sqrt{s} = 500$ GeV are given in fig. 5. The only difference with respect to the Lep 2 analysis is a smaller value for the jet separation parameter $y_{cut} = 0.001$. In particular no minimum angle between jets and either beam is required. A separation based on shape-variables of WW events from the background seems, at first sight, to be more difficult at the NLC than at Lep 2. Only for the angle between the two least energetic jets α_{34} the signal and background distribution are significantly different. The former peaks in the backward direction the latter is almost flat. On the contrary, the Bengtsson-Zerwas angle and the Körner-Schierholz-Willrodt angle distribution from CC11 are almost indistinguishable from those generated from the $q \bar{q} g g$ background. The sensitivity of the Nachtmann-Reiter angle is similar at

²Nagy and Trócsányi [7], however, find large corrections, of the order of 100% for the D parameter and for the acoplanarity.

the two energies. The signal distribution peaks at small angles, particularly at higher energies, while the background is flatter, with a large tail which extends to 180° . The distributions obtained in nQCD are closer to the full NLO results than at lower energies.

Conclusions

We have described the complete calculation of QCD radiative corrections to the process $e^+e^- \rightarrow u \bar{d} s \bar{c}$ which are essential in order to obtain theoretical predictions for W -pair production with per mil accuracy. The amplitudes we have derived are completely differential, and realistic cuts can be imposed on the parton level structure of the observed events. We have presented the distribution of the average reconstructed W -mass and the distribution of several four-jet shape variables at Lep 2 and NLC energies. The so called naive-QCD implementation of NLO corrections fails in both instances.

References

- [1] The most complete review of W -pair production at Lep 2 can be found in the Proceedings of the Workshop on Physics at Lep 2, G. Altarelli, T. Sjöstrand and F. Zwirner eds., Cern 96-01.
- [2] A. Ballestrero *et al.*, Determination of the mass of the W boson, in ref.[1], Vol. 1, p. 141.
- [3] The LEP Electroweak Working Group and the SLD Heavy Flavour Group, LEPEWWG/96-02.
- [4] E. Accomando *et al.*, DESY 97-100, hep-ph/9705442.
- [5] E. Maina and M. Pizzio, *Phys. Lett.* **B369** (1996) 341.
- [6] E. Maina, R. Pittau and M. Pizzio, *Phys. Lett.* **B393** (1997) 445.
- [7] J.M. Campbell, E.W.N. Glover and D.J. Miller, hep-ph/9706297;
E.W.N. Glover and D.J. Miller, hep-ph/9609474;
Z. Bern, L. Dixon, D.A. Kosower and S. Weinzierl, hep-ph/9609460;
A. Signer and L. Dixon, hep-ph/9609460;
A. Signer and L. Dixon, hep-ph/9706285;
Z. Nagy and Z. Trócsányi, hep-ph/9707309;
Z. Bern, L. Dixon and D.A. Kosower, hep-ph/9708239.
- [8] E. Accomando *et al.*, Event generators for WW physics, in ref.[1], Vol. 2, p. 3.
- [9] K.J. Abraham and B. Lampe, *Nucl. Phys.* **B478** (1996) 507.
- [10] A. Ballestrero and E. Maina, *Phys. Lett.* **B350** (1995) 225.
- [11] A. Ballestrero, in preparation.
- [12] G. Passarino and M. Veltman, *Nucl. Phys.* **B160** (1979) 151.
- [13] R. Pittau, *Comp. Phys. Comm.* **104** (1997) 23.
- [14] S. Catani and M.H. Seymour, *Nucl. Phys.* **B485** (1997) 291.
- [15] G.P. Lepage, *Jour. Comp. Phys.* **27** (1978) 192.
- [16] D. Bardin, D. Lehner and T. Riemann, *Nucl. Phys.* **B477** (1996) 27.
- [17] D. Bardin, M. Bilenky, A. Olchevski and T. Riemann, *Phys. Lett.* **B308** (1993) 403 [Erratum: **B357** (1995) 725].

- [18] S. Catani, Yu.L. Dokshitser, M. Olsson, G. Turnock and B.R. Webber, *Phys. Lett.* **B269** (1991) 432;
N. Brown and W.J. Stirling, *Z. Phys.* **C53** (1992) 629.
- [19] J. Fujimoto, T. Ishikawa, Y. Kurihara, Y. Shimizu, K. Kato, N. Nakazawa and T. Kaneko, hep-ph/9707260.
- [20] W. Beenakker, A.P. Chapovskii, F.A. Berends, CERN-TH-97-114, hep-ph/9706339;
W. Beenakker, A.P. Chapovskii, F.A. Berends, CERN-TH-97-158, hep-ph/9707326.
- [21] J.G. Körner, G. Schierholz and J. Willrodt, *Nucl. Phys.* **B185** (1981) 365;
O. Nachtmann and A. Reiter, *Z. Phys.* **C16** (1982) 45;
M. Bengtsson and P.M. Zerwas, *Phys. Lett.* **B208** (1988) 306;
M. Bengtsson, *Z. Phys.* **C42** (1989) 75;
S. Betke, A. Richter and P.M. Zerwas, *Z. Phys.* **C49** (1991) 59.
- [22] R. Barate *et al.*, ALEPH Coll., CERN-PPE/97-002.

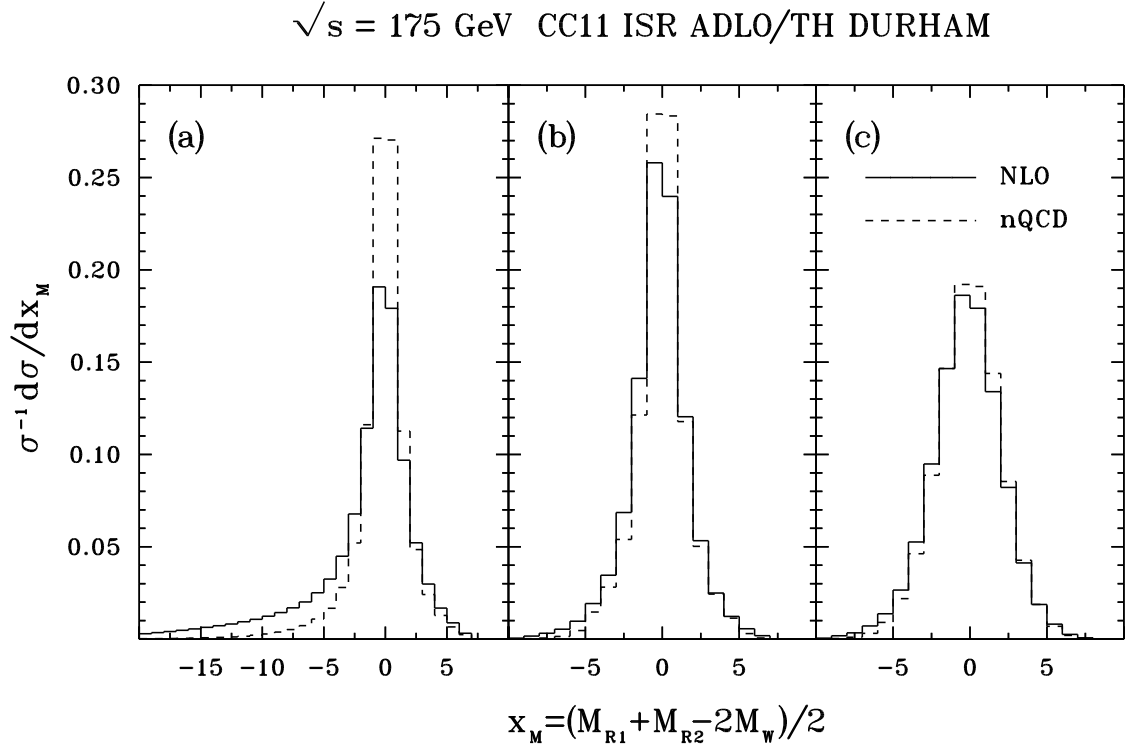


Fig. 2: Average mass distribution at $\sqrt{s} = 175 \text{ GeV}$. All ADLO/TH cuts are applied. The continuous histogram is the exact NLO result while the dashed histogram refers to nQCD. The corresponding cross sections can be found in table I.

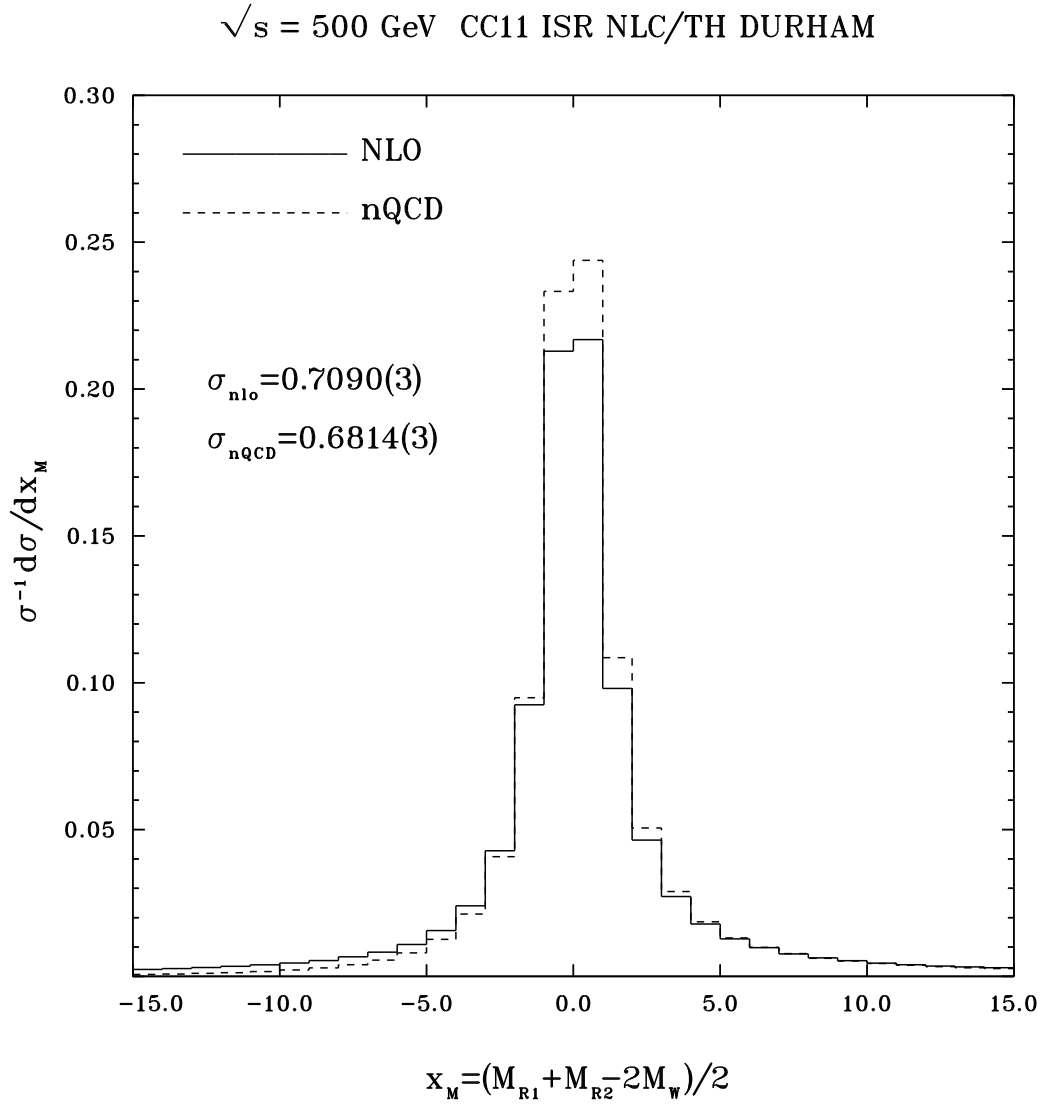


Fig. 3: Average mass distribution at $\sqrt{s} = 500 \text{ GeV}$. All NLC/TH cuts are applied. The continuous histogram is the exact NLO result while the dashed histogram refers to nQCD.

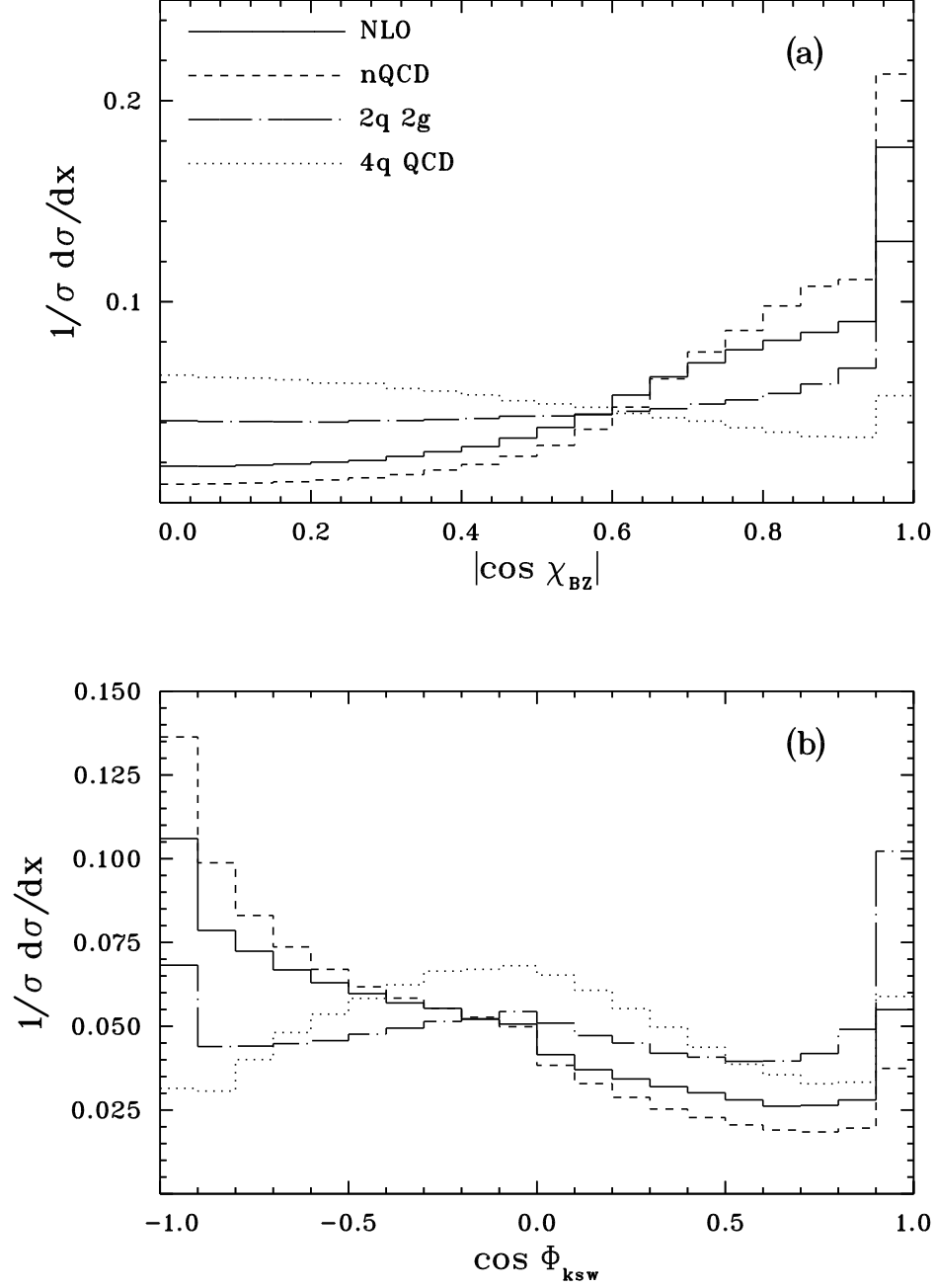


Fig. 4: The full NLO results (continuous line) is compared with the nQCD prediction (dashed line) and with the tree level background distributions from $q \, \bar{q} \, g \, g$ (chain-dotted line) and $q_1 \, \bar{q}_1 \, q_2 \, \bar{q}_2$ (dotted line).

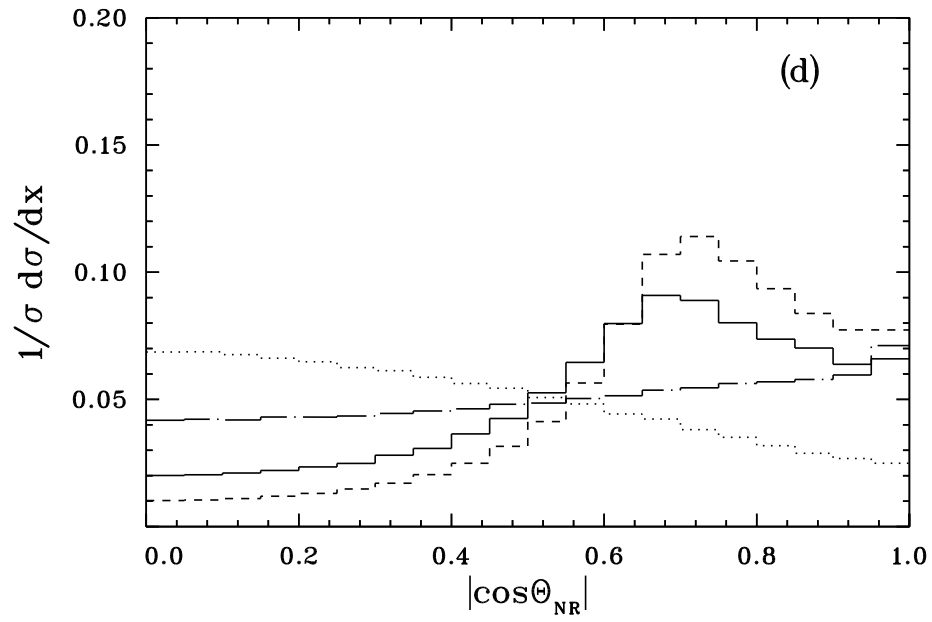
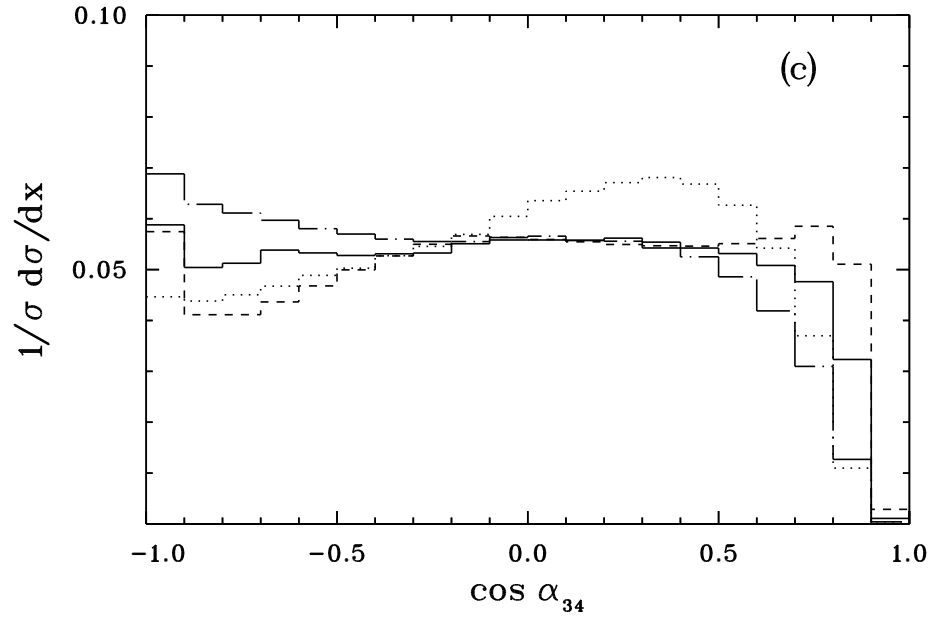


Fig. 4: Four-jet shape variables at $\sqrt{s} = 175$ GeV, continued.

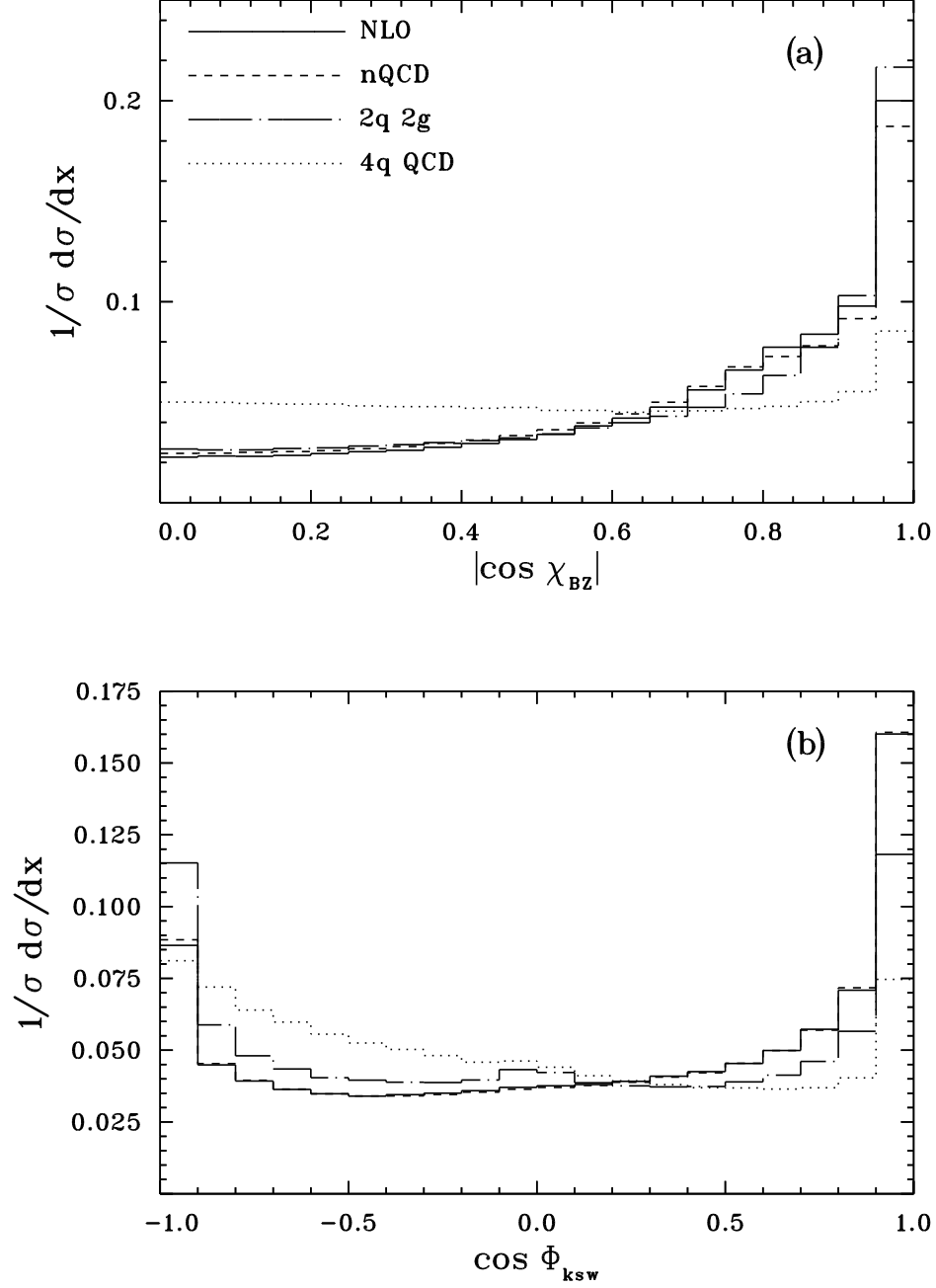


Fig. 5: Four-jet shape variables at $\sqrt{s} = 500$ GeV. The full NLO results (continuous line) is compared with the nQCD prediction (dashed line) and with the tree level background distributions from $q \, \bar{q} \, g \, g$ (chain-dotted line) and $q_1 \, \bar{q}_1 \, q_2 \, \bar{q}_2$ (dotted line).

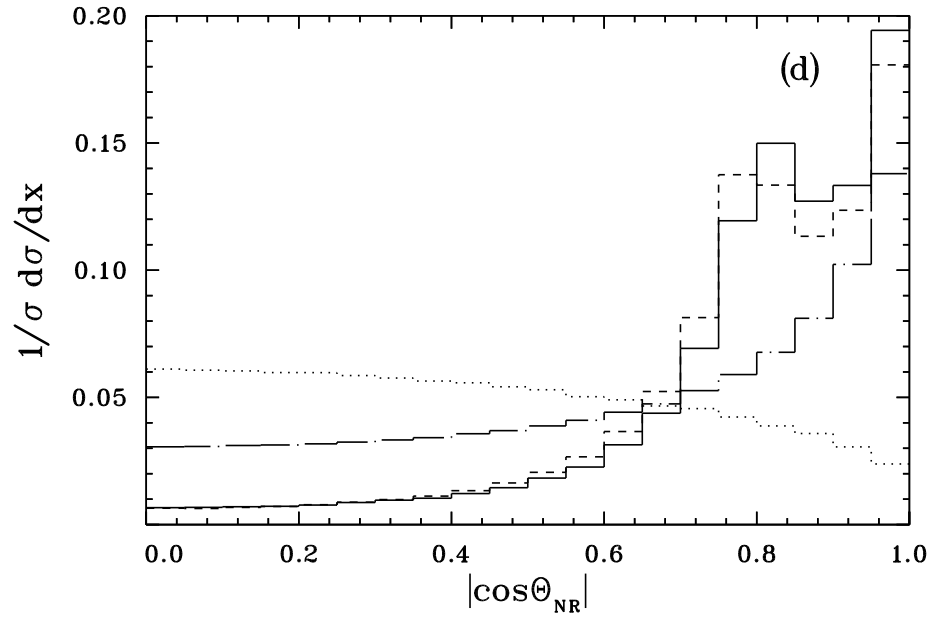
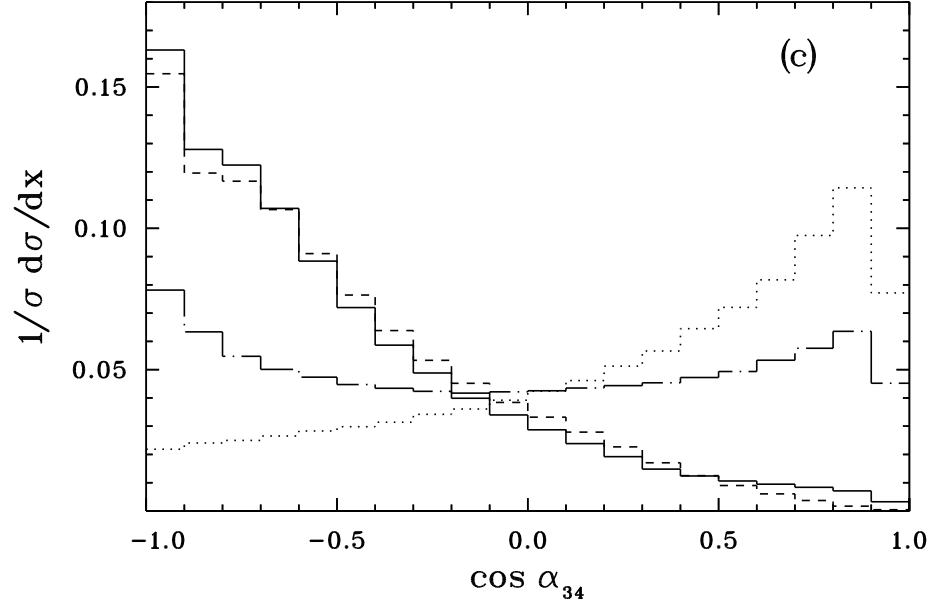


Fig. 5: Four-jet shape variables at $\sqrt{s} = 500$ GeV, continued.